Determining the Physical Properties of Near-Earth Objects

D. P. Cruikshank[1], J. P. Emery[1,2], A. K. Mainzer[3], S. P. Worden[1], E. Wright[4], P. Eisenhardt[5]

1. NASA Ames Research Center, Moffett Field, CA 94035-1000
2. SETI Institute,
3. Jet Propulsion Lab., Pasadena, CA 91129
4. Dept. of Astronomy, Univ. of California Los Angeles
5. Spitzer Science Center, California Inst. of Technology, Pasadena, CA

Abstract

Measurements of the thermal flux density of a near-Earth object (NEO) at a single wavelength gives an estimate of the dimensions of that object that has lower uncertainty than a similar measurement of the reflected sunlight in the visible spectral region. When the two measurements are combined, both the effective diameter and the geometric albedo can be derived. Thermal measurements at two or more wavelengths, plus the visual region flux density, give information on the thermal properties that are useful in evaluating the magnitude of the Yarkovsky effect. Recent observations of a modest sample of NEOs and theoretical modeling demonstrate that kilometer- and sub-kilometer size objects generally have insulating dust layers that are less extensive than on larger asteroids, but sufficient to cause a significant anisotropy to the emitted thermal radiation.

Introduction

The dimensions and thermal properties of near-Earth objects (NEOs) are parameters essential to an evaluation of the size-frequency distribution of their population(s) and the short-term orbital evolution of these bodies. The dimensions directly affect the energy dissipated in an impact with the Earth, while the orbital evolution affects issues central to the prediction and mitigation of impact. Dimensions and thermal properties can be derived from remote sensing observations made with telescopes on Earth and in space.

In this paper the term "asteroid" is understood to include objects of either asteroidal or cometary origin, both of which are encompassed in the term "near-Earth object" or NEO.

The anisotropic emission of thermal photons from a small asteroid exerts a force that is sufficient to cause the asteroid to spiral inward toward the Sun (if the rotation of the asteroid is retrograde) or outward (if the rotation is prograde). This phenomenon, called the Yarkovsky effect, results from the fact that the warmest portion of an asteroid's surface is the afternoon and early night region, in contrast to the morning and late night regions. Thus, more heat is radiated on the dusk side than on the dawn side, yielding a net force due to radiation pressure in the direction opposite to the dawn direction. This, the *diurnal* component of the Yarkovsky effect, is important in affecting the orbital evolution of asteroids in the approximate size range $0.1 < D < 10$ km (Vokrouhlický 1998). It has been measured in the asteroid 6489 Golevka from precision radar observations (Chesley et al. 2003). A *seasonal* component of the Yarkovsky effect is important primarily for objects smaller than 100 m in size and is not discussed further in this paper.

The Yarkovsky effect depends upon the thermal properties of the asteroid's surface, as well as other parameters (shape, surface roughness, spin rate, spin direction, etc.) because the thermal properties govern the rate at which a surface will heat from insolation and then radiate. The relevant thermal properties are thermal conductivity, temperature, and insulating properties of the uppermost surface layers; measurements that give information on these parameters will help evaluate the magnitude of the Yarkovsky effect for specific objects for which short-term orbital evolution may be important in influencing their potential as impact hazards.

Dimensions

Because the optical brightness of an asteroid depends on the product of its geometric albedo and projected area, its dimensions can be calculated from a measurement of its brightness in visible wavelengths only if the surface reflectance (albedo[1]) is known. Of the small sample of NEOs for which albedos have been measured (~40), albedos vary by more than a factor of ~30, from 0.023 to 0.63 (Stuart and Binzel 2004 and references therein). Since the size calculated from visible brightness depends on the square root of the albedo, the use of an assumption of the value of the albedo will result in an uncertainty of nearly a factor of six in the calculated size. In a survey of near-Earth objects in which the principal goal is to establish the dimensions of bodies posing a potential impact threat to Earth or of importance to the collisional history of the inner Solar System, it is inadequate to measure an object's optical brightness, assume the value of the albedo, and then depend on the calculated sizes in the ensuing scientific discussions.

Beyond an estimate made from an assumed albedo, the dimensions of an asteroid can be measured in a number of different ways, such as direct imaging (optical or synthetic imaging by radar), or multiple photometric measurement of the occultation of a star as an asteroid moves against the background of stellar objects. These techniques are applicable to only a handful of asteroids that have been visited by spacecraft, a few small bodies that have passed near the Earth, plus a selection of the largest main-belt asteroids.

A measurement of an asteroid's thermal flux near the wavelength of its blackbody emission peak (9 μm for an object of temperature 320 K) provides a more robust means of estimating size because thermal emission is not as strongly dependent on geometric albedo as the flux of reflected sunlight in the visible spectral region. The emitted flux is given by

$$F_\lambda = \frac{R^2}{\Delta^2} \int \varepsilon_\lambda B[\lambda, T(p_v)] \cos\theta_e \, d\Omega, \quad (1)$$

where F_λ is the flux at wavelength λ, R is the object radius, Δ is the object-observer distance, ε_λ is the emissivity at λ, $B[\lambda,T(p_v)]$ is the Planck function, θ_e is the emission angle (angle between the observer and surface normal; equal to incidence angle for phase=0^o), and $d\Omega$ is the incremental solid angle. The temperature (T) at any point on an asteroid's surface is dependent on the albedo at visible wavelengths (p_v) and the planetographic coordinates of that point. The integral is taken over the entire visible hemisphere of the object. In practice, solving Eq. 1 requires a model of the temperature distribution on the surface, which is determined by several parameters including its rotation rate, the orientation of its rotational pole with respect to the Sun, and

[1] The general term "albedo" is the ratio of the total reflected or scattered flux from a surface to the incident flux received from the Sun. The geometric albedo is the ratio of the flux at zero phase angle reflected from a surface relative to that expected from a Lambert sphere.

the composition and microstructural properties of its surface. These parameters are incorporated into a model that is most appropriate for the class of object under consideration.

A successful and commonly used model for NEOs, the Near Earth Asteroid Thermal Model (NEATM; Harris 1998), solves for radiative equilibrium at the sub-solar point ($T_{ss}=[S_o(1-p_vq)/r^2\sigma\varepsilon\eta]^{1/4}$, where S_o is the solar flux at 1AU, q is the phase integral, r is the distance from the Sun in AU, σ is the Stefan-Boltzmann constant, η is an empirical term called the beaming parameter, and ε is the bolometric emissivity) and assumes that the temperature varies as $\cos^{1/4}\theta_i$. It is further assumed that the nightside supplies no thermal emission. Along with R and p_v, three other parameters are not known *a priori*: ε, q, and η. Bolometric and 9 μm emissivities of silicate minerals that are dominant on asteroid surfaces are ~0.9 (e.g., Christensen *et al.* 2000, Salisbury *et al.* 1992). Emissivities do not exhibit much variation around this value, a few to ten percent at most, and therefore introduce negligible uncertainty in the resulting size estimate. Likewise, the phase integrals of asteroids cluster around 0.38 with small measured variations causing a similarly low level of uncertainty. The beaming parameter, η, however, which acts as a proxy of both surface roughness and thermal inertia (a measure of the resistance of the surface to changes in temperature--see below), can vary over factors of several (e.g., Delbo *et al.* 2003, Wolters *et al.* 2005). Lack of knowledge of p_v and η leads to uncertainty in the surface temperature, and dominates the uncertainties in size as estimated from a thermal flux measurement.

The NEATM uses measurements of thermal flux at two or more wavelengths to derive a color temperature, and the model temperature distribution is then adjusted by varying η until the model and observations are in accord. This parameter η is a measure of the deviation of the observed color temperature from that expected for a smooth spherical object with zero thermal inertia (Harris 2005).

Since the surface temperature depends only on the fourth root of the albedo, uncertainties in albedo propagate into much smaller uncertainties in the derived diameter than in the visible. The range of p_v and η that have been measured for NEOs (0.023-0.63 for p_v, 0.6-3.1 for η) result in maximum uncertainties of ~70% (or a multiplicative factor of 1.7 in either direction) in derived radius from a single band thermal measurement at 9 μm. This is not a 1-σ error, but a much more conservative estimate based on the full range of these parameters so far measured. A more accurate estimate of the 1-σ error of ~17% (factor of 1.17 in either direction) for diameter estimates comes from using the 1-σ uncertainties in p_v ($\langle p_v \rangle = 0.26 \pm 0.03$) and η ($\langle \eta \rangle = 1.65 \pm 0.15$).

Fig. 1 illustrates the technique and associated errors using simulated data. We used the orbit and size of a real NEO (1685 Toro; R=2.09 km) and simulated thermal fluxes at a single wavelength (9 μm) for detections on three nights (first observation and subsequent detections 5 and 30 nights later, representing one possible survey strategy), using the mean p_v and η listed above and assuming 7σ detections each night. We then fit the NEATM to all three dates, varying p_v and η either over their 1-σ ranges. For both objects, model fluxes with the reference R, $\langle p_v \rangle$, and $\langle \eta \rangle$ are shown by the solid lines. The different colors represent the different dates, and the dashed and dotted lines are the upper and lower limits. The 1-σ uncertainty in the derived radius estimate is a factor of ~1.17 (17%), which is significantly lower than the factor of ~2.3 (130%) uncertainty that would result from estimating the size from visible measurements without knowledge of the albedo.

The addition of another wavelength of measurement in the thermal infrared, allowing the calculation of a color temperature, will constrain the models and the derived physical parameters more tightly. The value of the second wavelength in thermal observations of Kuiper Belt objects with the *Spitzer Space Telescope* is demonstrated in papers by Cruikshank et al. (2005) and Stansberry et al. (2006).

When thermal detections, either from space or from the ground, are accompanied by concurrent measurements of the reflected sunlight, the two measurements can be combined to derive the albedo and size simultaneously, and thereby further reduce the size uncertainty arising from a single measurement. Allen (1970) first developed the technique for measuring the dimensions of asteroids and other airless solid bodies in the Solar System using the measured flux of reflected sunlight at visible wavelengths plus the thermal flux measured in the infrared spectral region. This *radiometric technique* gives a quantitative measure of effective radius, as well as the albedo of the solid body. It has been calibrated against asteroids for which direct measurements of the dimensions are available from imaging, radar, and occultation data, and was the basis for the dimensions and albedos published in the IRAS asteroid survey (Tedesco et al. 1992, 2002).

The basic radiometric method to obtain an effective radius, *R*, and geometric albedo, *p*, is to solve two equations with these two unknowns (Allen 1970; Matson 1972; Morrison 1973; Lebofsky and Spencer 1989), Eq. 1 for the thermal flux and

$$F_{vis} = \frac{S_o}{r^2} R^2 p_v \frac{\Phi_{vis}}{\Delta^2}, \qquad (2)$$

for the visible reflected flux, where Φ_{vis} is the (dimensionless) phase function in the visible spectral region (related to q and derived from the IAU H, G formalism (Lumme & Bowell 1981)); all other parameters are as defined previously. The beaming parameter, η, has been determined for a number of asteroids using measurements of their thermal fluxes and the standard thermal model (STM) for their surface thermal properties.

For this study, co-author J. Emery used *Spitzer Space Telescope* spectral observations (5 - 35 μm) of eight near-Earth asteroids and calculated the value of η for each, using NEATM. The mean is 1.32 and the standard deviation in the mean is 0.19.

Thermal Inertia

The thermal inertia of a surface, or its resistance to a change in temperature, is important in evaluating the magnitude of the diurnal Yarkovsky effect (Vokrouhlický 1998), because it plays a pivotal role in the temperature distribution and the anisotropy of the emission of thermal radiation that applies a small force affecting the orbital evolution of small bodies, as noted above. Thermal inertia, Γ, is given by $(\kappa\rho c)^{0.5}$, where κ is the thermal conductivity, ρ is the density, and C is the specific heat; the units are J m^{-2} $s^{-0.5}$ K^{-1}. In the absence of information on the surface roughness, spin orientation, and non-sphericity of an NEO, the value of η alone is insufficient to derive the thermal inertia. However, through modeling of observations, preferably at two or more thermal wavelengths, Γ can be derived with a reasonable degree of confidence.

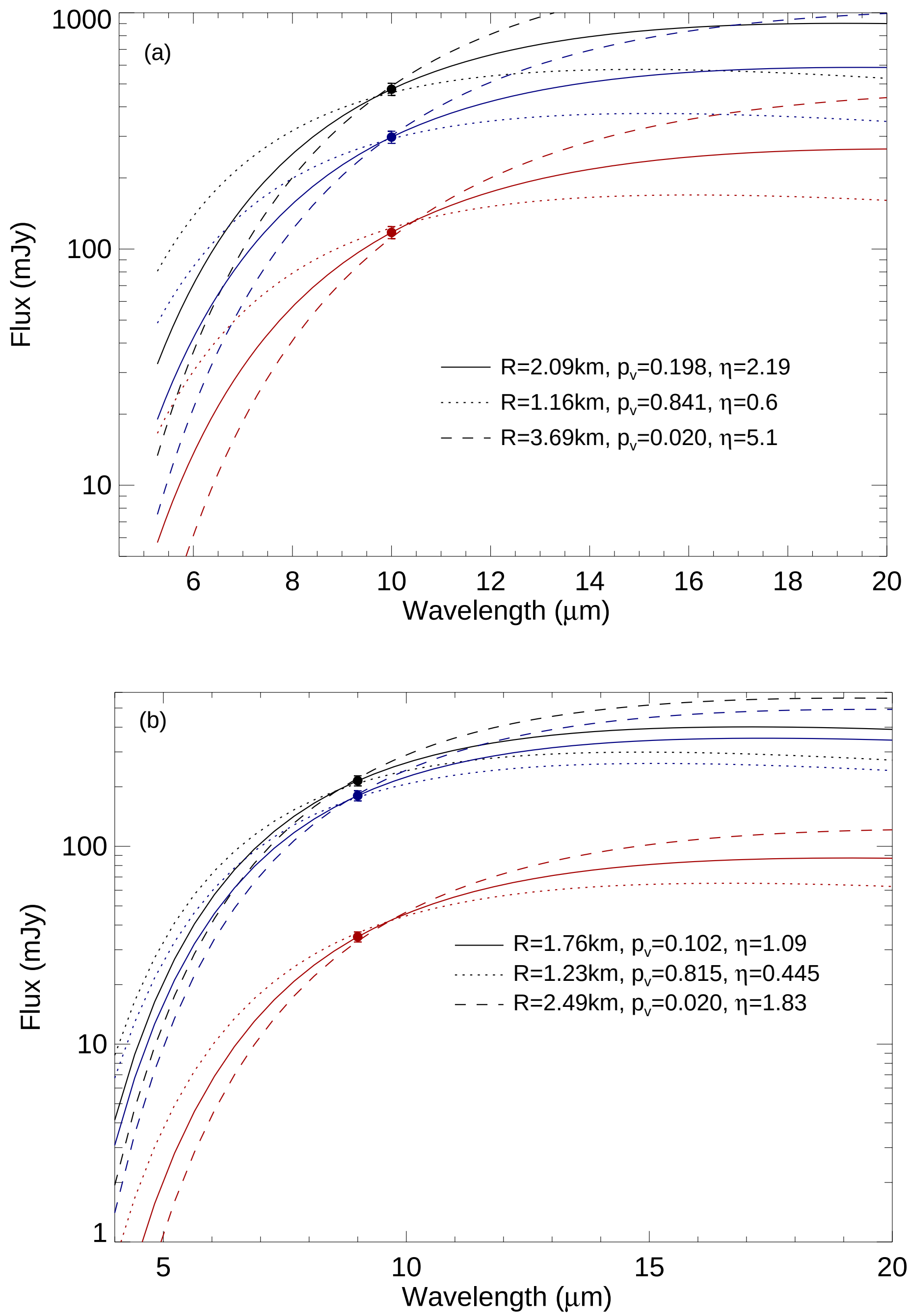

Fig. 1. *Illustration of radius estimates and associated uncertainties from NEOCam detections. The simulated data and object positions in (a) are derived from Spitzer/IRS observations of 1685 Toro, and those in (b) from Spitzer/IRS observations of 7092 Cadmus. The different colors represent different dates (second and third observations are separated by 5 and 30 nights, respectively, from the first observation). The radius is the derived quantity, and the dotted and dashed lines are lower and upper limits to the models that fit the data, allowing* p_V *and* η *to range to the extremes of their plausible values.*

The dimensionless thermal parameter, $\Gamma\omega^{0.5}/\sigma T_{ss}^{3}$, where ω is the angular velocity of the asteroid's rotation, σ is the Stephan-Boltzmann constant, and T_{ss} is the temperature of the subsolar point, is useful to demonstrate the effect of the thermal inertia; the Yarkovsky effect is maximum when the value of this parameter is 1 or 2.

Harris (2005) has summarized thermal inertia determinations from thermal modeling of three NEOs as follows: (433) Eros [effective diameter 17.5 km] Γ ~ 150; (1580) Betulia [effective diameter 4.5 km] Γ ~ 180; (25143) Itokawa [effective diameter ~0.3 km] Γ ~ 350 (see Fig. 2). For comparison, five main belt asteroids with diameters >200 km have values of Γ in the range 5-25 J m^{-2} $s^{-0.5}$ K^{-1}. For bare rock Γ ~ 2500, for Mars 40<Γ<650, and for the Moon Γ ~50 J m^{-2} $s^{-0.5}$ K^{-1}. For the high-albedo Kuiper Belt object (55565) 2000 AW197, Cruikshank et al. (2005) estimated Γ ~ 9 in the same units.

Harris (2005) used the NEATM to derive the best-fit value of η for a sample of about 40 observations of small NEOs, plotting the dependence of η on solar phase angle (Fig. 3). The mean value from the 41 points in this figure is η = 1.50 (max value 3.1, min value 0.75) [these values are estimated graphically, giving each point equal weight, from the data points in the figure].

As noted by Harris (2005), the distribution of values of η in Fig. 3 suggests that most NEOs have lower thermal inertias than that of bare rock, but greater than the lunar regolith, indicating the presence of a thin and patchy insulating layer of finely powdered material. The sparse insulating layer and bare rock outcrops generally enhance the anisotropy of emitted thermal radiation, and thereby amplify the importance of the Yarkovsky effect in the orbital evolution of these bodies.

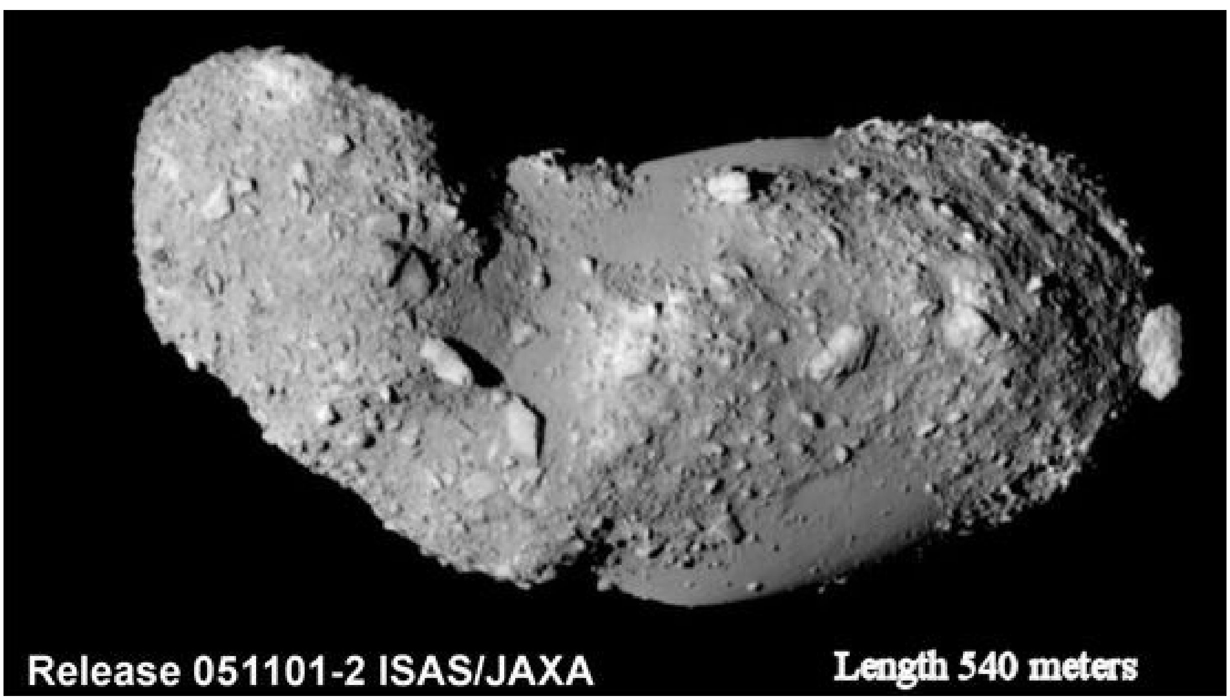

Fig. 2. Apollo asteroid (25143) Itokawa imaged with the Hyabusa spacecraft. Note the patchy distribution of dust and the large exposed boulders.

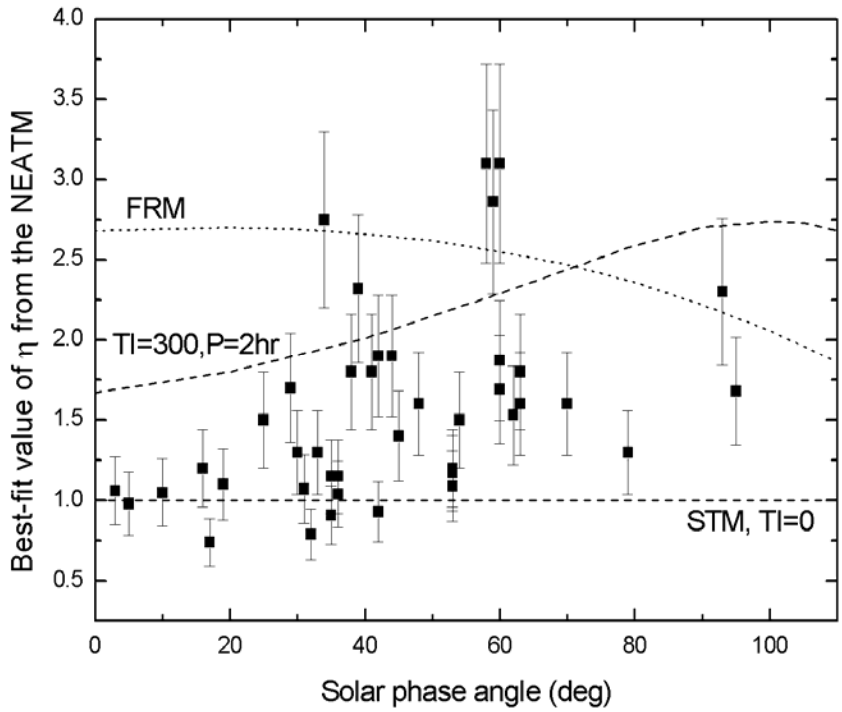

Fig. 3. *Best-fit values of η from the NEATM of a set of NEOs with adequate multi-filter photometric data to enable η to be derived from spectral fitting. Where the same object was observed at different phase angles, multiple points are shown. The dashed line at η = 1 is the lower limit given by an STM-type asteroid (zero thermal inertia or spin axis pointing at the Sun) with a smooth surface. The curve labeled FRM is an upper limit for a population of fast rotation/high thermal inertia, e.g., bare rock asteroids. The dashed curve represents the upper limit for a population of spherical, smooth asteroids at 1 AU from the Sun with thermal inertia = 300 $Jm^{-2}s^{-0.5}K^{-1}$ and rotation periods longer than 2 hrs. Figure courtesy A. W. Harris (Harris 2005).*

Summary

To obtain reliable information on the dimensions and thermal properties of large numbers of NEOs in a survey mode, a combination of observations at visible and thermal wavelengths has proven to be effective, despite remaining uncertainties for individual objects about their spin axis orientation, surface roughness, and shape. Statistical studies of the most important parameters, although based on small samples, show that kilometer and sub-kilometer size bodies have thin and patchy powdered regoliths, less extensive than that of the Moon, but significantly different from bare rock. Objects of special interest discovered in a survey could be targeted for longer term observations that would yield the spin axis information required for more detailed investigations of the thermal properties. The dimensions of objects observed three times in a single thermal region wavelength can be derived with reasonable accuracy, while concurrent flux density measurements at visual wavelengths and at additional thermal wavelengths significantly enhance the accuracy of the calculated dimensions and albedos, and also yield the thermal properties of the surface.

Acknowledgments This material was developed as a part of a proposal for a NEO detection and measurement mission submitted by the Jet Propulsion Laboratory to the 2006 Discovery Program. We have especially benefited from the discussion in the recent paper by A. W. Harris (2005).

References

Allen, D. 1970. Infrared diameter of Vesta. *Nature 227*, 158.

Chesley, S. R., Ostro, S. J., Vokrouhlický, D., Capek, D., Giorgini, J. D., Nolan, M. C., Margot, J.-L., Hine, A. A., Benner, L. A. M., and Chamberlin, A. B.). *Science 302*, 1739-1742.

Christensen, P.R., Bandfield, J.L., Hamilton, V.E., Howard, D.A., Lane, M.D., Piatek, J.L., Ruff, S.W., Stefanov, W.L. 2000. A thermal emission spectral library of rock forming minerals. *J. Geophys. Res. 105(E4)*, 9735-9739.

Cruikshank, D. P., Stansberry, J. A., Emery, J., P., Fernández, Y. R., Werner, M. W., Trilling, D. E., and Rieke, G. H. 2005. The high-albedo Kuiper Belt object (55565) 2002 AW_{197}. *Astrophys. J. 624*, L53-L56.

Delbo, M., Harris, A.W., Binzel, R.P., Pravec, P., Davies, J.K. 2003. Keck observations of near-Earth asteroids in the thermal infrared. *Icarus 166*, 116-130.

Fernández, Y. R., Jewitt, D., and Sheppard, S. 2002. Astron. J. 123, 1050-1055

Harris, A.W. 1998. A thermal model for near-Earth asteroids. *Icarus 131*, 291-301.

Harris, A. W. 2005. The surface properties of small asteroids from thermal-infrared observations. In Proc. IAU Symp. 229, *Asteroids, Comets, Meteors* (D. Lazzaro, S. Ferraz-Mello, & J. A. Fernández, eds.), Cambridge University Press, Cambridge, pp. 449 -463.

Lebofsky, L. A., and Spencer, J. R. 1989. Radiometry and thermal modeling of asteroids. In *Asteroids II* (R. P. Binzel, T. Gehrels, and M. S. Matthews, eds.). Univ. Ariz. Press (Tucson), 128-147.

Lumme, K, and Bowell, E. 1981. Radiative transfer in the surfaces of atmosphereless bodies. I - Theory. II - Interpretation of phase curves. *Astron. J. 86*, 1694-1721.

Matson, D. L. 1972. Ph.D. Thesis, California Institute of Technology

Morrison, D. 1973. Determination of radii of satellites and asteroids from radiometry and photometry. *Icarus 19*, 1-14.

Salisbury, J.W., Walter, L.S., Vergo, N., D'Aria, D.M. 1992. *Mid-infrared (2.1 – 25 μm) spectra of minerals*. 346 pp., Johns Hopkins Univ. Press, Baltimore, MD.

Stansberry, J. A., Grundy, W. M., Margot, J. L., Cruikshank, D. P., Emery, J. P., Rieke, G. H., and Trilling, D. E. 2006. The albedo, size, and density of binary Kuiper Belt Object. (47171) 1999 TC_{36}. *Astrophys. J. 643*, 556-566

Stuart, J.S. and R.P. Binzel 2004. Bias-corrected population, size distribution and impact hazard for the near-Earth objects. *Icarus 170*, 235-311.

Tedesco, E. F., Veeder, G. J., Fowler, J. W., and Chillemi, J. R. 1992. *The IRAS minor planet survey* (Phillips Lab. Tech. Report PL-TR-92-2049). Hanscom AFB, MA: Phillips Lab. Dir. Geophys. Air Force Materiel Command. 437 pp.

Tedesco, E. F., Noah, P. V., Noah, M., and Price, S. D. 2002. The supplemental IRAS minor planet survey. *Astron. J. 123*, 1056-1085.

Vokrouhlický, D. (1998). Diurnal Yarkovsky effect as a source of mobility of meter-sized asteroidal fragments. I. Linear theory. *Astron. & Astrophys. 335*, 1093-1100.

Wolters, S.D., Green, S.F., McBride, N., Davies, J.K. 2005. Optical and thermal infrared observations of six near-Earth asteroids in 2002. *Icarus 175*, 92-110.